ACS Sustainable Chemistry & Engineering

Research Article

pubs.acs.org/journal/ascecg

Mathematical Modeling of Fast Biomass Pyrolysis and Bio-Oil Formation. Note II: Secondary Gas-Phase Reactions and Bio-Oil Formation

Eliseo Ranzi,* Paulo Eduardo Amaral Debiagi, and Alessio Frassoldati

Dipartimento di Chimica, Materiali e Ingegneria Chimica "Giulio Natta", Politecnico di Milano, Piazza Leonardo da Vinci, 32, 20133 Milano, Italy

Supporting Information

ABSTRACT: This paper summarizes the research activities done at Politecnico di Milano in the field of the detailed kinetic modeling of fast pyrolysis of biomass to produce bio-oil. Note I of this work already discussed biomass characterization and the multistep pyrolysis mechanisms of reference species. The model is able to provide a detailed composition of pyrolysis products and char residue. Different critical steps are involved in this multicomponent, multiphase and multiscale problem. The first complexity relies in biomass characterization. Then, fast pyrolysis process involves detailed kinetic mechanisms, first in the solid phase for the biomass pyrolysis, then in the gas-phase for the secondary reactions of released products. The complexity of these kinetic mechanisms requires strong simplifications, thus chemical lumping procedures are extensively applied. Successive or secondary gas phase reactions of gas and tar components released during the pyrolysis process complement the kinetic model, together with the heterogeneous reactions of residual char. The modeling of fast pyrolysis process requires a comprehensive description of the coupled transport and kinetic processes, both at the particle and the reactor scale. A few examples and comparisons with experimental data validate the reliability of the overall model. Finally, the composition and physical properties of the pyrolysis bio-oil are also discussed, with emphasis on combustion and pollutant emissions.

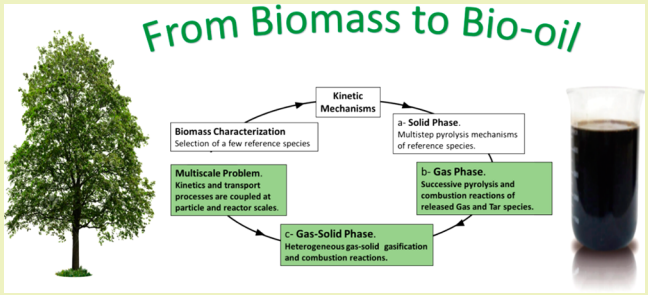

KEYWORDS: *Fast pyrolysis process, Detailed mechanism of biomass pyrolysis, Secondary gas-phase reactions of biomass pyrolysis products, Multiscale modeling of biomass pyrolysis, Bio-oil combustion properties*

1. INTRODUCTION

Although Note I of this work already presented the biomass characterization based on a few reference species together with their pyrolysis mechanisms,[1] the main subject of this paper is to complete the modeling steps required for the description of fast biomass pyrolysis to produce bio-oil, with particular attention to the chemistry of this process. Figure S1 in the Supporting Information very schematically shows a fast pyrolysis process with a circulating fluidized bed reactor.[2] Biomass is dried and grinded to reduce the moisture and to improve both the fast heating of small biomass particles and the quality of the bio-oil. Combustion of gas and char produced in this process can supply the required pyrolysis heat. Bio-oil obtained after condensation of the tar products is typically a dark red-brown liquid, highly polar, with high density ~1200 kg/m^3.

Although the endothermic pyrolysis reaction requires a high rate of heat transfer and adequate times, the residence time of released volatiles must be short enough to avoid successive decomposition reactions. High heating rates improve bio-oil production, whereas low heating rates favor biochar formation. High pyrolysis temperatures supported by catalyst and oxidizing atmospheres are used for syngas production. Biomass pretreatments allow significant improvements of pyrolysis process.[3] Currently, bubbling and circulating fluidized bed processes produce bio-oil on a commercial scale, using woody biomasses. Circulating fluidized bed reactors are suitable for larger throughputs with respect to bubbling reactors, even though hydrodynamics is more complex.[2]

The graphical abstract highlights the multicomponent, multiphase, and multiscale nature of biomass pyrolysis and also shows the relevant role of chemistry in this process. After the first pyrolysis of the biomass particle, the chemistry also affects the evolution of thermal reactors with the heterogeneous reactions of residual char, and mainly with the successive gas-phase reactions of pyrolysis products, i.e., gas and tar species. The coupling of chemical kinetics and transport phenomena needs to be considered both at particle and reactor scale in order to account for the correct temperature and time distributions. A further complexity arises from the anisotropic nature of the biomass particles and from fractures and

Received: December 19, 2016
Revised: February 20, 2017
Published: February 22, 2017

DOI: 10.1021/acssuschemeng.6b03098
ACS Sustainable Chem. Eng. 2017, 5, 2882−2896

comminutions of biomass particles during the pyrolysis process. Thermo and transport properties of biomass and char also vary with the conversion progress and the modeling of fast pyrolysis process requires well-balanced efforts.[4]

One of the peculiarities of the biomass pyrolysis mechanism described in Note I of this work,[1] and here attached as Table S1 in the Supporting Information, is its ability to provide a detailed composition of pyrolysis products and char residue. The overall kinetic model also requires the heterogeneous reactions of biochar, as well as the secondary gas phase reactions of gas and bio-oil species released during biomass pyrolysis. The large kinetic mechanism of these secondary gas phase pyrolysis and combustion of hydrocarbon and oxygenated species takes great benefit from a firm experience in pyrolysis[5] and combustion kinetics.[6]

After this Introduction, the Secondary Gas-Phase Reactions of Released Products section describes the secondary gas-phase reactions of volatile species released during biomass pyrolysis. Namely, three major reaction classes of successive reactions are analyzed: chain radical reactions, molecular dehydration reactions, and successive reactions of aromatics species to form heavy poly aromatic hydrocarbons (PAH) and soot. The Heterogeneous Reactions of Residual Char section shortly discusses the heterogeneous reactions of char gasification and combustion. The Mathematical Model at the Particle and the Reactor Scale section presents the mass and energy balances at the particle and reactor scale. Bio-Oil Production and Comparisons with Experimental Data analyzes the bio-oil formation in terms of yields and composition. The Bio-Oil Composition and Combustion Properties section discusses the challenging features of bio-oil combustion related to material compatibility, flame stability, and emissions. Finally, some conclusions are drawn in Conclusion section, together with a critical discussion not only on advantages and limits of the present model but also on how new experimental and theoretical work can be useful to improve further the knowledge of this process.

SECONDARY GAS-PHASE REACTIONS OF RELEASED PRODUCTS

Primary volatile products released from biomass pyrolysis are often exposed to high temperatures, where gas phase reactions play a significant role.[7−9] Thus, it is possible to find optimal operating temperature and conditions corresponding to maximum bio-oil yield because of secondary gas-phase reactions, which are responsible for bio-oil reduction with increase of gas yields.[2,10−13] An extension of a general kinetic mechanism of pyrolysis and combustion of hydrocarbon and oxygenated fuels[14] is very useful for describing these successive reactions of tar and gas species. Because of the modular structure of detailed kinetic mechanisms, their extension simply requires to include the primary reactions of the new species released from biomass pyrolysis. These are chain initiation, H-abstraction and addition reactions, together with molecular and successive radical decomposition, until the formation of intermediates already considered in the kinetic mechanism. The complete POLIMI kinetic mechanism in CHEMKIN format, together with thermodynamic properties of all involved species, is provided as Supporting Information. The overall dimensions of the kinetic scheme, in terms of species and reactions, is a compromise between model accuracy and computational efforts. For this reason, a few lumped components represent and group several tar and heavy species and/or isomers with similar reactivity. As a simple example, the free fatty acid (FFA: $C_{18}H_{32}O_2$) released by the triglycerides groups the unsaturated fatty acids and is a combination of methyl-linoleate ($C_{19}H_{32}O_2$) and methyl-decanoate ($C_{11}H_{18}O_2$) with a mole ratio 0.875/.125, which satisfies the atomic balances. These components are already considered in POLIMI mechanism of pyrolysis and oxidation of heavy methyl esters.[15]

As already mentioned, three major reaction classes of successive reactions are here considered: chain radical reactions, molecular dehydration reactions, and successive reactions of aromatics species to form PAH.

Chain Radical Reactions: Generic Rate Rules of Initiation and H-Abstraction Reactions. Because of the large number of successive reactions of volatiles from biomass pyrolysis, Carstensen and Dean[7] already highlighted that it is not feasible to perform ab initio calculations of rate constants for all the reactions. From first principle calculations, they systematically derived rate estimation rules, to be extrapolated inside the same reaction class. Similarly, in modeling steam cracking reactions, Dente et al.[5,16] highlighted that the rate constant of initiation and H-abstraction reactions of pure hydrocarbons are obtained, with reasonable accuracy, by adopting generic rate rules based on bond dissociation energy (BDE) of the reacting molecules.

Favored chain initiation reactions involve the breaking of the weakest bonds. From microscopic reversibility principle, rate constant of initiation reactions are derived from the rate constant of the reverse radical recombination reaction. If the activation energy of the radical recombination is zero, the activation energy of the reverse unimolecular dissociation reaction becomes directly the BDE.

Rate of H-abstraction or metathesis reactions depend on the reference rate constant of the different abstracting radicals and on the type of H atoms to be abstracted.[17] Table 1 reports a series of BDEs of different C−H bonds in hydrocarbon and oxygenated species. These BDE values highlight that all radicals can easy abstract allyl and acyl H atoms, because of the lower

Table 1. C−H Bond Dissociation Energy (kcal/mol) of Hydrocarbon and Oxygenated Species Calculated at G4 Level (298 K)

$CH_3-CH_2-CH_2-C\underline{H}_3$	*n*-butane	99.7	Primary H atom in alkanes
$CH_3-CH_2-C\underline{H}_2-CH_3$	*n*-butane	97.2	Secondary H atom in alkanes
$(CH_3)_3-C\underline{H}$	iso-butane	95.4	Tertiary H atom in alkanes
$CH_2=CH-C\underline{H}_3$	propylene	85.9	Primary allyl H atom in alkenes
$CH_2=CH-C\underline{H}_2-CH_3$	1-butene	83.3	Secondary allyl H atom in alkenes
$C\underline{H}_2=CH-CH_2-CH_3$	1-butene	109.3	Primary vinyl H atom in alkenes
$CH_2=C\underline{H}-CH_2-CH_3$	1-butene	105.9	Secondary vinyl H atom in alkenes
$CH_3-CH_2-CH_2-C\underline{H}_2-OH$	1-butanol	93	Primary α H atom in alcohols
$CH_3-CH_2-C\underline{H}_2-CH_2-OH$	1-butanol	98.2	Secondary β H atom in alcohols
$CH_3-CH_2-CH_2-C\underline{H}O$	*n*-butanal	87.5	Acyl H atom in aldehydes
$CH_3-CH_2-C\underline{H}_2-CHO$	*n*-butanal	89.2	Secondary β H atom in aldehydes

DOI: 10.1021/acssuschemeng.6b03098
ACS Sustainable Chem. Eng. 2017, 5, 2882−2896

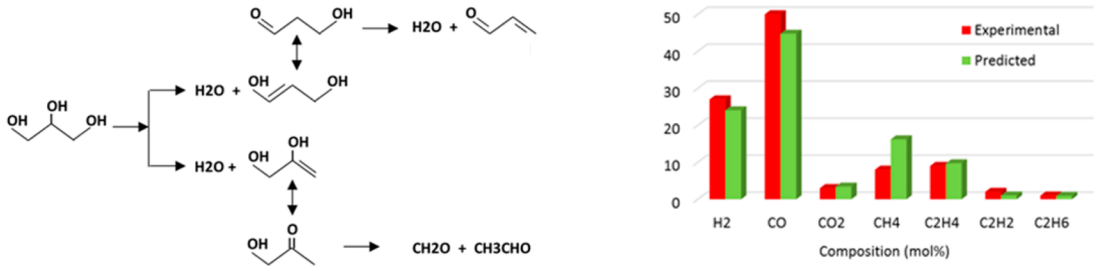

Figure 1. Glycerol pyrolysis. (Left Panel) Successive water elimination reactions. (Right Panel) Glycerol pyrolysis at 800 °C and 1 atm. Comparisons of experimental data[26] and model predictions.

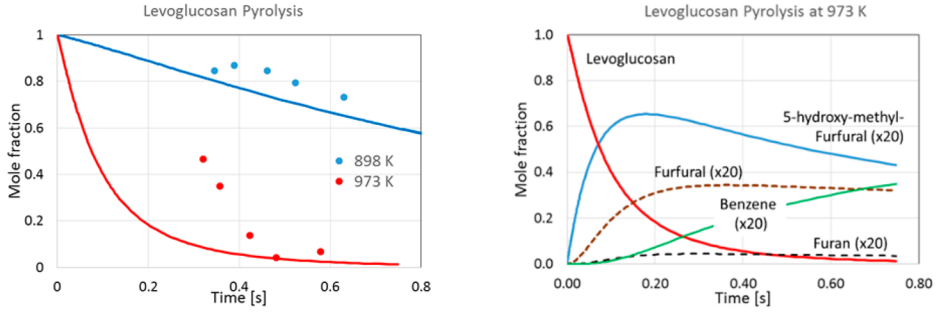

Figure 2. Levoglucosan pyrolysis in a flow reactor.[28] (Left Panel) Levoglucosan fractions at 898 and 973 K. (Right Panel) Successive decomposition reactions of LVG and predicted yields of 5-hydroxymethyl-furfural, furfural, furan, and benzene at 973 K.

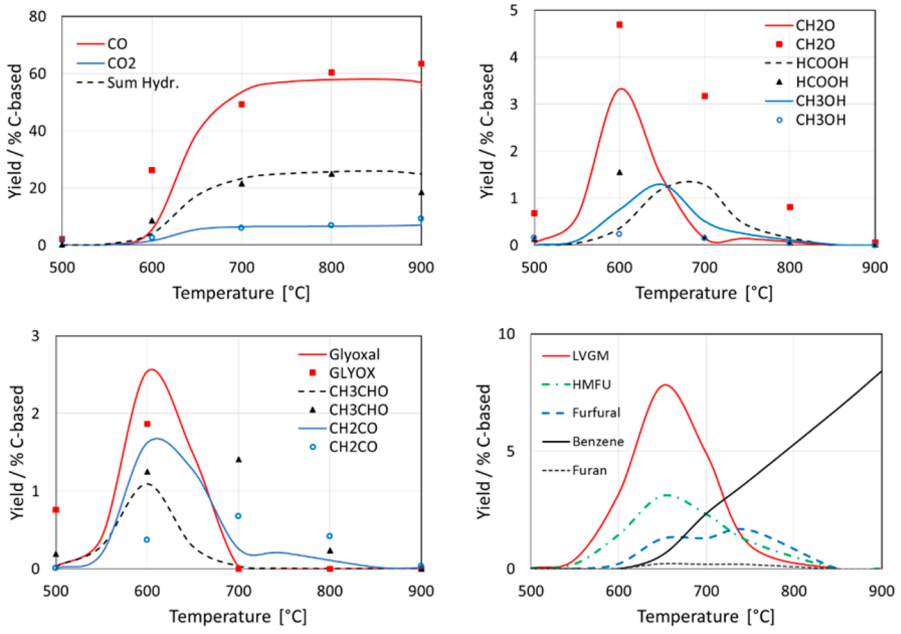

Figure 3. Pyrolysis of levoglucosan.[32] Comparisons between experimental data (symbols) and model predictions (lines).

BDEs, whereas the removal of vinyl H atoms is more difficult. Figure S2 in the Supporting Information compares the rates constants of H-abstraction of H, OH, and CH_3 radicals from primary, secondary, tertiary, allyl, and vinyl positions. Similar generic rate rules are derived for H-abstraction reactions in oxygenated species.[18]

These rate rules, both for initiation and H-abstraction reactions, are very useful to define a first reasonable set of rate parameters of secondary gas phase radical reactions.

Molecular Reactions and Water Elimination Reactions: Alcohols, Glycerol, and Carbohydrates. It is well-defined the importance of water elimination and molecular reactions in cellulose and biomass pyrolysis.[19−21] Dehydration reactions will be here sequentially discussed moving first from simple alcohols, then through glycerol and levoglucosan, to 5-hydroxymethyl-furfural.

Figure S3 shows the four center molecular dehydration reactions of 2-butanol to form 1-butene and 2-butene.[22,23] OH position inside the carbon skeleton[24] slightly affects reference rate parameters of this reaction class, whereas large differences are observed for substituted aldehydes, when water eliminations form unsaturated species with conjugated double bonds. Figure 1 shows the two successive dehydration reactions in glycerol pyrolysis.[25]

DOI: 10.1021/acssuschemeng.6b03098
ACS Sustainable Chem. Eng. 2017, 5, 2882−2896

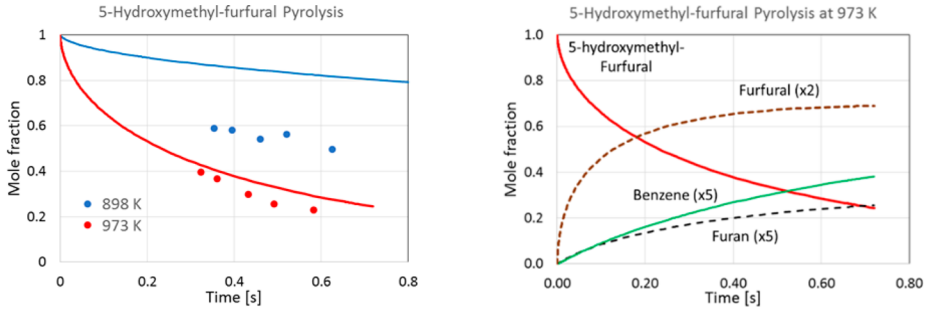

Figure 4. 5-Hydroxymethyl-furfural pyrolysis in a flow reactor at 898 and 973 K.[28] (Left Panel) Comparisons of experimental data (symbols) and model predictions (lines). (Right Panel) Predicted successive decomposition products.

The first dehydration reaction again refers to previous reference rate parameters:

$$\text{glycerol} \rightarrow \text{1propene1, 3-diol} + H_2O$$
$$k = 0.210^{14} \exp(-65000/RT)\ [s^{-1}]$$

Then, the keto−enol tautomerism transforms 1propene1,3-diol into 3-hydroxypropanal, which rapidly forms acrolein through a second dehydration reaction. The aldehyde moiety strongly influences the reactivity and it stabilizes the transition state and the products with a reduction of the activation energy of more than 10 kcal/mol:[7]

$$\text{3-hydroxy-propanal} \rightarrow \text{acrolein} + H_2O$$
$$k = 10^{14} \exp(-51000/RT)\ [s^{-1}]$$

Fukutome et al.[26] studied glycerol pyrolysis up to 800 °C and residence times of 0.9−1.4 s. Figure 1 compares experimental and predicted gas composition at 800 °C, where conversion of glycerol and intermediate products was nearly complete. Syngas products are slightly underestimated, whereas an opposite deviation was observed by Fantozzi et al.[25] with respect to similar experimental data of glycerol pyrolysis.[27]

Dehydration reactions rule the first molecular decomposition of carbohydrates, specifically of levoglucosan and xylan. Successive levoglucosan dehydration reactions form the 5-hydroxymethyl-furfural ($C_6H_6O_3$: HMFU), whose successive reactions form furfural ($C_5H_4O_2$) and furfuryl-alcohol ($C_5H_6O_2$).[28,29] Retro-Diels−Alder reactions are further molecular reactions forming C_2−C_4 oxygenated species.[7] Chain initiation and H-abstraction reactions are also considered with the usual rules, well-defined for hydrocarbon and oxygenated species.[5,16,30] Primary radicals progressively decompose forming major intermediates, such as formaldehyde, hydroxyl-acetaldehyde, glyoxal, acetol, and small-oxygenated components.

Figure 2 compares model predictions and experimental data of levoglucosan (LVG) decomposition at 898 and 973 K.[28] The same figure also shows the evolution of 5-hydroxymethyl furfural, furfural, and furan, together with the successive benzene formation.

Kawamoto et al.[31] and Fukutome et al.[26,32] studied the reactivity of levoglucosan, glyceraldehyde (CH_2OH−$CHOH$−CHO), and acetol (CH_3−CO−CH_2OH) in a tubular reactor at 400−900 °C and residence times 0.8−1.4 s. Figure 3 compares model predictions and experimental data of major gas and condensable species. Although C_4−C_6 species are not measured, an overall selectivity of ∼10% is predicted, because of successive dehydration reactions to form 5-hydroxy-methyl-furfural, furfural and furan. The kinetic model predicts a relevant formation of benzene, which is mainly formed via propargyl radical recombinations.

To validate further the kinetic model, Figure 4 compares predictions and experimental data of 5-hydroxymethyl-furfural (HMFU) pyrolysis at 898 and 973 K.[28] Predicted yields of furfural, furan are also reported, together with benzene formation. Molecular and a radical reaction path of HMFU form furfural, which in turn decomposes to furan, via H abstraction and CO elimination. Furan pyrolysis has been experimentally[33] and theoretically investigated[34] More recently, the kinetics of furan and furan derivatives received a particular attention.[35−37] Principal pyrolysis products are CO and propyne as a major channel, and C_2H_2 and ketene. Again, benzene is mainly formed through recombination reactions of propargyl radicals.

Successive Reactions of Aromatics and Phenolics To Form Polycyclic Aromatic Hydrocarbons. Phenolic species deserve a special attention, not only for their presence as tar components released by lignins but also as possible precursors of dibenzofurans and dibenzodioxins. Kinetic studies on phenol, cresol, and anisole chemistry highlighted the importance of CO elimination from unsubstituted and substituted phenoxy radicals both with a molecular path:

$$C_6H_5O \rightarrow cyC_5H_5 + CO$$
$$k = 5.10^{11} \exp(-43920/RT)\ [s^{-1}]$$

and with radical reactions to form CO and cyclopentadienyl radicals.[7,9] Although phenol and cresol were extensively investigated for their interest in combustion systems, anisole ($C_6H_5OCH_3$) was mainly studied as a surrogate of tar from lignin pyrolysis.[38−40] These studies highlighted the importance of the ipso-addition reactions, whose reference rate parameters are derived from these simple reactions:

$$H + \text{Anisole} \rightarrow \text{Phenol} + CH_3$$
$$k = 1.10^{13} \exp(-6000/RT)\ [cm^3/s/mol]$$

$$H + \text{Phenol} \rightarrow \text{Benzene} + OH$$
$$k = 1.210^{13} \exp(-6000/RT)\ [cm^3/s/mol]$$

$$H + \text{Anisole} \rightarrow \text{Benzene} + OCH_3$$
$$k = 1.10^{13} \exp(-8000/RT)\ [cm^3/s/mol]$$

$$OH + \text{Toluene} \rightarrow \text{Cresol} + H$$
$$k = 1.110^{12} \exp(-11000/RT)\ [cm^3/s/mol]$$

DOI: 10.1021/acssuschemeng.6b03098
ACS Sustainable Chem. Eng. 2017, 5, 2882−2896

Table 2. Primary Volatile Products Released from Fast Pyrolysis of Lignin at 0.1 s

	Experimental			Predicted		
	Gas Phase (0.1 s)			Prim. Pyrolysis + 0.1 s of secondary reactions		
Temperature [K]	773	1023	1223	773	1023	1223
Products (wt %)						
H_2	0.0	0.3	1.2	0.0	0.3	1.3
CO	1.0	15.0	33.1	8.7	16.8	32.5
CO_2	4.5	6.4	8.3	5.5	5.7	6.6
CH_4	1.2	4.1	6.7	0.7	2.3	6.3
C_2	0.3	2.5	3.6	2.9	4.1	5.8
C_3−C_5	0.3	3.5	0.4	0.0	0.4	0.8
Aromatics (C_6+)	0.2	3.3	8.4	1.1	2.2	6.2
Light Oxygenated	5.7	3.8	0.1	7.5	6.1	1.2
Phenolics[a]	28.0	14.2	4.5	15.5	15.6	4.1
H_2O	7.6	6.8	6.2	6.2	7.2	7.5
Total Volatiles	48.7	60.0	72.3	48.1	60.6	72.1
Char[a]	51.2	39.6	27.6	51.9	39.2	27.9
C (wt %)	75.30	80.90	97.70	78.04	85.61	99.98
H (wt %)	3.60	3.00	2.30	4.39	3.12	0.02
O (wt %)	21.10	16.00	0.00	17.57	11.27	0.00

[a]With 50% of undetectable products added (see text).

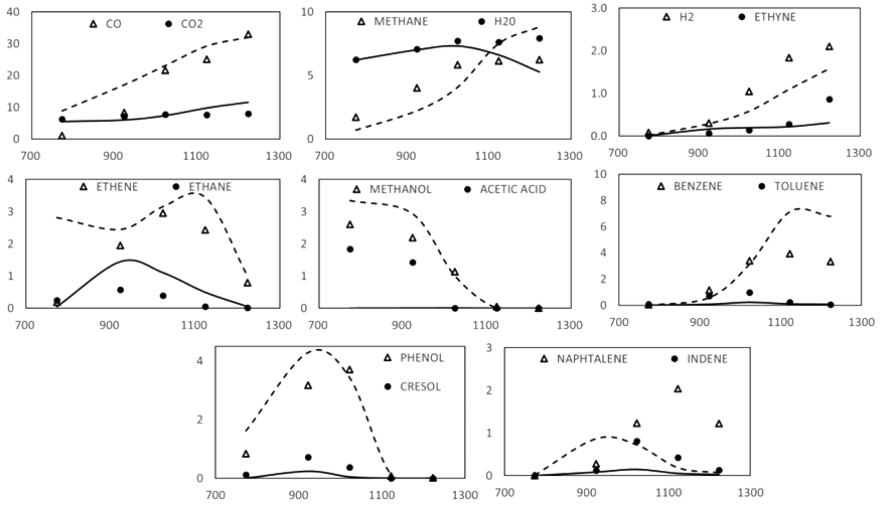

Figure 5. Weight fractions of volatile species released from lignin pyrolysis at different temperatures [K] with residence time of 3.6 s in the second tubular reactor. Comparison between experimental data[49] (symbols) and model predictions (lines).

$$OH + Toluene \rightarrow Phenol + CH_3$$

$$k = 4.410^{12} \exp(-6700/RT)\ [cm^3/s/mol]$$

$$CH_3 + Phenol \rightarrow Cresol + H$$

$$k = 1.\ 310^{12} \exp(-16200/RT)\ [cm^3/s/mol]$$

All these reactions progressively convert the aromatic and phenolic species.[41]

Recently, Norinaga et al.[42] discussed the reaction pathways to form benzene, toluene, and naphthalene from levoglucosan and cellulose pyrolysis. The formation of aromatics from the high temperature biomass pyrolysis is largely due first to the recombination of propargyl radicals, then to successive addition reactions of acetylenic species. Since several years, the formation mechanisms of polycyclic aromatic hydrocarbons and soot have been extensively investigated.[43,44] POLIMI kinetic mechanism was recently revised and improved in this area.[45,46]

Secondary Gas-Phase Reactions of Volatiles from Lignin Pyrolysis. Norinaga et al.[42,47] developed a two-stage tubular reactor for studying first the fast biomass pyrolysis and then the secondary reactions of pyrolysis products at residence times up to 6 s in a wide temperature range. These data were useful for validating the secondary gas-phase reactions of released species.[48] The model correctly predicts the time evolution of the major gas products as well as the decomposition of tar and intermediate species, properly accounting for benzene and toluene formation.

More recently, Yang et al.[49] investigated the secondary reactions of volatiles derived from the fast lignin pyrolysis at 500−900 °C, and 241 kPa. The lignin sample, prepared by enzymatic hydrolysis (EHL), has the elemental C/H/O composition 63.5/5.93/30.57, on a dry basis. A large amount of heavy undetectable phenolic species (>30% at 773 K) were obtained from the fast EHL pyrolysis in the first reactor. Table 2 reports the primary volatile products released from fast pyrolysis of lignin as experimentally measured after 0.1 s.[49] Very

DOI: 10.1021/acssuschemeng.6b03098
ACS Sustainable Chem. Eng. 2017, 5, 2882−2896

Table 3. Bio-Char Gasification and Combustion Reactions (units: kcal, kmol, m^3, K, s)

Reaction	k
Char + O_2 → CO_2	$1.2 \times 10^{10} \exp(-32300/RT)$ [Char][a] [O_2]
Char +0.5 O_2 → CO	$2.5 \times 10^{11} \exp(-38200/RT)$ [Char] [O_2]$^{0.78}$
Char + H_2O → CO + H_2	$2.5 \times 10^{9} \exp(-52000/RT)$ [Char]$^{0.5}$ [H_2O]$^{0.70}$

[a]Note that [Char] is here considered as the ratio of actual Char to initial Char concentration.

heavy phenolic species are not considered in the kinetic model, because of the lumping approach. Therefore, we corrected the experimental data by assuming the undetected heavy species as equally distributed between the phenolic species and char residue. Predicted pyrolysis products as obtained from lignin pyrolysis after 0.1 s are also reported and they show an overall reasonable agreement with experimental data. At high temperatures, the effect of secondary gas phase reactions is a significant decomposition of intermediates to form CO and H_2, and a relevant formation of aromatics, up to heavy PAHs. The oxygen and hydrogen content in the char residue, as a function of the pyrolysis temperature, well agrees with experimental measurements.

Figure 5 compares experimental and model predictions of volatile species released from lignin pyrolysis at different temperatures with residence time of 3.6 s in the second tubular reactor.[49] The predicted values were obtained by directly feeding the lignin (EHL) to the two-stage tubular reactor. After the first pyrolysis stage, primary pyrolysis products were fed to the second tubular reactor with the residence time of 3.6 s. The reasonable agreement confirms the predictive feature of the whole pyrolysis model, i.e. it is not necessary to use the experimental information on the primary decomposition products from lignin. In fact, the direct and coupled use of primary biomass pyrolysis products together with successive gas-phase reactions gives satisfactory predictions. Further details on these calculations are reported elsewhere.[9] Again, model results indicate in a predictive way the formation of ∼5% of polyaromatic hydrocarbon species heavier than C_{20}, in agreement with the experimental observation of soot deposition on reactor walls above 1023 K.

HETEROGENEOUS REACTIONS OF RESIDUAL CHAR

The carbon content of residual char increases rapidly with temperature, being typically in the range of 85−95% (wt %) at high temperatures. This goes with a loss of oxygen and hydrogen, which decrease to 15−5% and <2%, respectively.[50]

Di Blasi[12] critically analyzed the rate laws and kinetic constants for the gasification and the combustion of chars produced from biomass pyrolysis. She also discussed the role played on char reactivity by various factors, such as feedstock, heating rate, temperature, pressure, and composition of the inorganic matter. A reduced graphitization and a larger surface area are the reasons of a higher char reactivity with the decrease in the external pressure. Asadullah et al.[51] studied the structural features and combustion reactivity of chars prepared from the fast pyrolysis using Raman spectroscopy and thermogravimetric analysis. They observed that the formation of amorphous carbon structure with smaller polyaromatic rings are dominant in chars from thick particles at low temperatures, whereas char from small particles at higher temperatures favors the formation of larger aromatic ring systems. The former structures are more reactive than the latter ones. The presence of inorganic catalytic species also plays an important role in char reactivity. However, the char structure seems to play a more dominant role than the catalytic effects in char reactivity. In fact, although higher char surface area improves the reactivity, pore size distribution and diffusion limitations in micropores affect the catalyst activity and apparent reactivity.[52] As a result, the catalytic activity of alkali and alkaline earth metallic species is dependent on their interaction with char structure.[53]

Heterogeneous gas−solid reactions of the residual char are mainly of interest in combustion and gasification process, whereas they are of limited importance in pyrolysis process. Although fundamental and more detailed discussions can be found elsewhere,[4,12,54−56] Table 3 summarizes some reference kinetic parameters of major char combustion and gasification reactions.[57,58]

MATHEMATICAL MODEL AT THE PARTICLE AND THE REACTOR SCALE

When pyrolysis of thick biomass particles is modeled, the coupling of chemical kinetics with intra- and interphase heat and mass transfer resistances is required. A convenient way to present mass and energy balance equations is to discuss particle and reactor scale.[4]

Particle Scale. The particle model predicts the time evolution of temperature and concentration profiles inside the particle. Biomass particles shrink even more than 50% during their conversion. Reliable rules for estimating the variations of transport properties during the pyrolysis process are a need, because they affect heat transfer processes.[11] Energy and continuity equations govern the temperature and concentration gradients inside the particles. Isotropic spherical particles are assumed and they are discretized into N sectors.

The mass balances of solid and gas phase are

$$\frac{dm_{j,i}^{S}}{dt} = V_j R_{j,i} \tag{1}$$

$$\frac{dm_{j,i}}{dt} = J_{j-1,i} S_{j-1} - J_{j,i} S_j + V_j R_{j,i} \tag{2}$$

where $m_{j,i}$ and $m_{j,i}^{S}$ are the mass of the i^{th} volatile and solid component; t is the time variable; V_j is the volume of the j^{th} sector;$R_{j,i}$ is the formation rate of i^{th} component of biomass pyrolysis mechanism.[1] Finally, S_j is the external surface and J are the total fluxes generated by diffusion and pressure gradients.

The energy balance is

$$\frac{d\sum_{i=1}^{NCP} m_{j,i}^{S} h_{j,i}}{dt} = JC_{j-1} S_{j-1} - JC_j S_j + S_{j-1} \sum_{i=1}^{NCG} J_{j-1,i} h_{j-1,i} - S_j \sum_{i=1}^{NCG} J_{j,i} h_{j,i} + V_j HR_j \tag{3}$$

where $h_{j,i} = c_{P_{j,i}} T_j$ is the component partial enthalpy; T_j is the temperature of the j^{th} sector. The term JC accounts for the heat conduction; the term $V \times HR$ accounts for the total reaction

DOI: 10.1021/acssuschemeng.6b03098
ACS Sustainable Chem. Eng. 2017, 5, 2882−2896

heat; NCP and NCG are the total number of solid and gas components.

Solid species are constrained to remain inside the sector, and only mass exchange of volatile species between adjacent sectors is allowed. Density, shrinking, and porosity of each particle sector are evaluated as the sum of all the corresponding property.

Fick, Fourier, and Darcy laws rule mass and heat fluxes within the particle:

$$J_{j,i} = -D_{j,i}^{\text{eff}} \text{MW}_i \frac{\mathrm{d}c_{j,i}}{\mathrm{d}r}\bigg|_{r_j} - \frac{\text{Da}_j}{\mu_j}\frac{\mathrm{d}P_j}{\mathrm{d}r}\bigg|_{r_j} c_{j,i}\text{MW}_i \tag{4}$$

$$\text{JC}_j = -\kappa_j^{\text{eff}} \frac{\mathrm{d}T_j}{\mathrm{d}r}\bigg|_{r_j} \tag{5}$$

where $D_{j,i}^{\text{eff}}$ and K_j^{eff} are the effective diffusivity and conductivity; MW and c are the molecular weight and the concentration; r is the radius; Da is the Darcy coefficient; μ is the viscosity of the gas phase and P is the pressure.

Boundary conditions at the gas−solid interface are

$$J_{N,i} = k_{\text{ext}}\text{MW}_i(c_{N,i} - c_i^{\text{bulk}}) + \frac{\text{Da}_N}{\mu_N}\frac{\Delta P}{\Delta r}\bigg|_N c_{N,i}\text{MW}_i \tag{6}$$

$$\text{JC}_N = h_{\text{ext}}(T_N - T^{\text{bulk}}) + \text{JR}_N + \sum_i^{\text{NCG}} J_{N,i}h_{N,i} \tag{7}$$

where k_{ext} and h_{ext} are the convective transfer coefficients[4] and JR_N is the net radiation heat.

A simple application example at the particle scale refers to the pyrolysis of thick biomass particles. The center temperature profiles of thick biomass particles show the presence of two thermal regimes during pyrolysis. The temperature first increases until reaching a plateau at 350−400 °C and then the temperature increases further, even exceeding the external pyrolysis temperatures. The plateau is due to the endothermic release of tar components, whereas the temperature peak shows the exothermic nature of the charification processes. Several sets of experimental measurements confirm this behavior.[59] Figure 6 shows a comparison between experimental and predicted profiles.[60] The behavior of these temperature profiles is highly sensitive to the thermochemical properties of the biomass pyrolysis, as well as to the biomass content of cellulose, hemicellulose, and lignins. Further model details and validation examples are reported in Corbetta et al.[48]

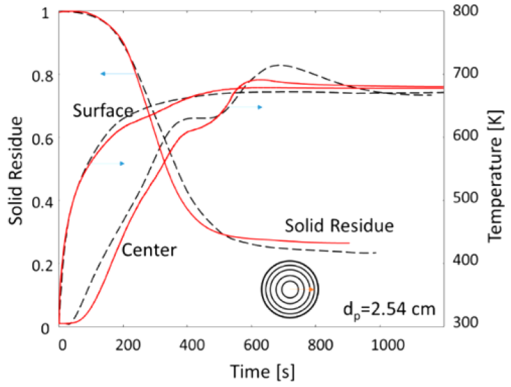

Figure 6. Temperature profiles and solid residue in a wood sphere of 2.54 cm.[60] Experiments (dashed lines) and model predictions (solid lines).

Reactor Scale. Although the mathematical model of fluidized bed or entrained bed reactors can directly refer to the previous particle model, the definition of an elemental reactor layer describing the gas−solid interactions is useful for the modeling of fixed bed reactors, which can be simulated as a series of several elemental layers. The height of each layer is of the same order of the size of the biomass particle, accounting for the vertical dispersion phenomena.

The gas-phase mass balance equations for each elemental reactor are

$$\frac{\mathrm{d}g_i}{\mathrm{d}t} = G_{\text{in},i} - G_{\text{out},i} + J_{N,i}S_N\eta + V_{\text{R}}R_{\text{g},i} \tag{8}$$

where g_i is the mass of i^{th} species within the reactor volume V_{R}; $G_{\text{in},i}$ and $G_{\text{out},i}$ are the inlet and outlet flow rate; $R_{\text{g},i}$ is the net formation of i^{th} species from secondary gas-phase reactions; the term $J_{N,i}$ is the gas−solid mass exchange multiplied by the particle surface S_N and the number h of particles inside the layer. Accordingly, the gas-phase energy balance for each elemental reactor is

$$\frac{\mathrm{d}\sum_{i=1}^{\text{NCG}} g_i h_{g_i}}{\mathrm{d}t} = \sum_{i=1}^{\text{NCG}} G_{\text{in},i}h_{g_{\text{in},i}} - \sum_{i=1}^{\text{NCG}} G_{\text{out},i}h_{g_i} + \sum_{i=1}^{\text{NCG}} J_{N,i}h_{N,i}S_N\eta + h_{\text{ext}}(T_N - T^{\text{bulk}})S_N\eta + V_{\text{R}}\text{HR}_{\text{g}} \tag{9}$$

where $h_{\text{g},i} = c_{P_i}T^{\text{bulk}}$; T^{bulk} is the gas-phase temperature; $G \times h_{\text{g}}$ are the enthalpies of inlet and outlet flow rates; $J \times h$ is the enthalpy flux relating to the mass transfer of a single particle; finally HR_{g} is the overall heat of gas-phase reactions. The reactor index is not reported in eqs 8 and 9. Boundary conditions and closure equations characterize different reactor configurations. Further details on these balance equations, including comments on the numerical methods to solve the overall system, are given in Ranzi et al.[61]

BIO-OIL PRODUCTION AND COMPARISONS WITH EXPERIMENTAL DATA

Gas, tar and residual char are the products of biomass pyrolysis, but their proportions are greatly dependent on biomass nature and process operating conditions. Torrefaction, pyrolysis, and gasification are three modes of thermal treatments of biomass, depending on heating rate, temperature, and residence times. Table S3 of Supporting Information summarizes different pyrolysis and gasification processes and gives operating conditions, time scales, and product yields.[2]

Low temperatures (300−500 °C) and long residence times of gas and tar released by biomass characterize slow pyrolysis and maximize biochar production. Tar species go through cross reticulation and condensation reactions and favor secondary char formation. High heating rates and short residence times distinguish fast pyrolysis. The bio-oil yield can reach 60−70 wt %, whereas even higher values are obtained in flash pyrolysis.[3] Thick particles (3−6 cm), pellets, and biomass briquettes in packed bed reactors are usual biomass feed for slow pyrolysis, whereas small particles in fluidized bed reactors are typical for fast heating process.[11,12] Moderate temperatures and short vapor residence times optimize bio-oil yields, whereas more

DOI: 10.1021/acssuschemeng.6b03098
ACS Sustainable Chem. Eng. 2017, 5, 2882−2896

severe conditions favor the successive conversion of tar species to syngas production.[2,10,62] Small particles give higher liquid yields, but they are costly to grind. Torrefaction, which is a thermal treatment under mild pyrolytic conditions, is useful for improving energy density and biomass grindability.[63,64]

The heart and crucial portion of the fast pyrolysis process is the reactor, and great research efforts are focused on developing new reactor configurations. Bridgwater[2] reports a widespread review of fast pyrolysis reactors, discussing their major features.

- Bubbling fluid beds are a proved technology, which is simple in construction and operation, with efficient heat transfer and good temperature control. Char product is ∼15 wt % and can be used to provide the pyrolysis heat.
- Circulating fluid bed and transported bed reactors are similar to the previous ones, except that char, vapors, and gas have a similar residence time. Because of the high velocities, char attrition can become a negative issue.
- The rotating cone reactor effectively operates as a transported bed reactor, but with transport effected by centrifugal forces in a rotating cone rather than gas.[65]
- In ablative pyrolysis, heat is transferred from the hot reactor wall to the wood surface. The pyrolysis front moves through the biomass particle, and the reaction rate is strongly dependent on the pressure of wood onto the heated surface.
- The auger pyrolysis reactor is characterized by a double-screw, where chopped biomass is mixed with hot sand and decomposed to vapors and char.
- Hydropyrolysis combines pyrolysis and hydrocracking by adding hydrogen in order to reduce the oxygen content of bio-oil product.
- Microwave heating and pyrolysis is largely different from the previous techniques as the biomass particles are rapidly heated from within. The interesting aspect is the absence of thermal gradients and the possibility of studying fundamentals of fast pyrolysis kinetics.

At the commercial scale, a key issue in the optimal reactor design is the way to provide the process heat from the combustion of char or gas byproduct, or from fresh biomass.[66]

A couple of comparisons with experimental data allows to verify model predictions and mainly the model sensitivity to process conditions related to the heating of biomass particles and to the residence time of pyrolysis products.

Flash Pyrolysis of Pine Sawdust in a Conical Spouted Bed Reactor: Effect of Heating of Biomass Particles. Aguado et al.[67] studied the flash pyrolysis of sawdust with N_2 in a conical spouted bed reactor at 350−700 °C and 50 ms of gas residence time. They studied the effect of pyrolysis temperature on the yields and composition of gas, liquid, and char, assuming a residence time of biomass particles of ∼10 min.[68] A maximum liquid yield of ∼70 wt % was observed at 450 °C. Proximate analysis of the sawdust was: fixed carbon = 16.04; volatile matter = 83.74; ash = 0.22. The ultimate analysis is C/H/O = 44.80/6.56/48.49; with N = 0.05, and S = 0.1 (in wt %). According to this analysis and assuming 5 wt % of moisture, the biomass characterization method described in Note I of this work[1] gives the following detailed composition of reference species:

CELL = 0.516	HCELL = 0.226 (glucomannans)	
LIGH = 0.136	LIGO = 0.011	LIGC = 0.041
TGL = 0.012	TANN = 0.002	Moisture = 0.050

Figure 7 compares experimental data and model predictions in terms of organic oil, water, gas, and residual char. Although a maximum liquid yield of 70 wt % is properly predicted, large deviations are observed at low temperatures. These deviations highlight the importance of the residence time of solid particles, i.e., of their thermal resistances and heating time. By halving the residence time from 10 to 5 min, it is possible to reduce strongly the observed deviations, at low temperatures. This effect, here observed by reducing the residence time of the solid particles, could be also due to the presence of biomass particles with larger sizes, i.e., requiring more time to complete the devolatilization process. Predicted profiles for a residence time of 2 min are also reported in order to complete the sensitivity analysis to the heating of biomass particles.

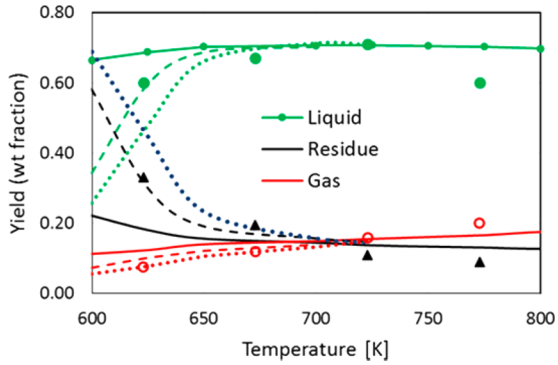

Figure 7. Fast pyrolysis of pine sawdust.[64] Effect of biomass residence time: 10 min (solid lines), 5 min (dashed), and 2 min (dotted). Comparisons of experimental data (symbols) and model predictions of bio-oil (including water), gas, and residual char vs reactor temperature.

Fast Pyrolysis of Pine Wood Particles in a Fluidized-Bed Reactor: Effect of Secondary Gas-Phase Reactions. Westerhof et al.[69] treated pine wood particles in a small fluidized bed fast pyrolysis reactor at 330−580 °C. Pine wood particles of 1 mm, a density of 570 kg/m^3, and a moisture content of 9−10 wt % were used, together with silica sand particles of 250 μm as fluidized bed material. The bio-oil yield initially increases up to ∼56−58 dry wt %, then is nearly constant at 450−530 °C, and finally decreases at higher temperatures. Biomass biochemical composition was given as cellulose/hemicellulose/lignin = 35/29/28, with a ultimate analysis C/H/O = 46.58/6.34/46.98 (wt %, daf), with traces of N and S, and 2.6 wt % of ash.

Figure 8 compares experimental data and model predictions in terms of organic oil, water, gas, and residual char. The residence time of the solid particles is 5 min, whereas only 1 s is assumed for the released gas and tar species. The largest deviations are observed at temperatures higher than 800 K. By assuming a gas residence time of 5 s, it is possible to account for these deviations. The secondary gas-phase reactions significantly reduces these deviations by decomposing organics in favor of gas yields, at temperatures higher than 800 K. As already discussed in the previous example, the low temperature deviations can be explained based on a lower residence time of the solid particles, or on a size distribution involving large diameters.

Both these examples refer to fast pyrolysis of a softwood biomass; consequently, model predictions are similar. Maximum liquid yield is about 65−70 wt %, with 10−15% of water, as a global value due to the initial moisture and the pyrolysis

DOI: 10.1021/acssuschemeng.6b03098
ACS Sustainable Chem. Eng. 2017, 5, 2882−2896

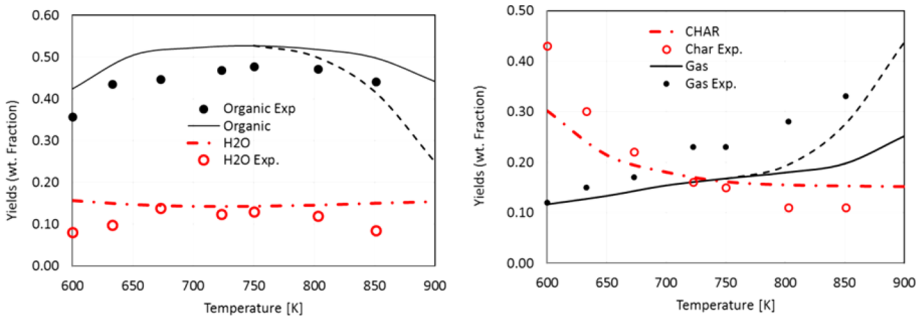

Figure 8. Pine wood pyrolysis. Effect of secondary gas phase reactions. Comparisons between experimental data and model predictions[69]. Predictions for gas residence time 1 s (solid lines) and 5 s (dashed lines).

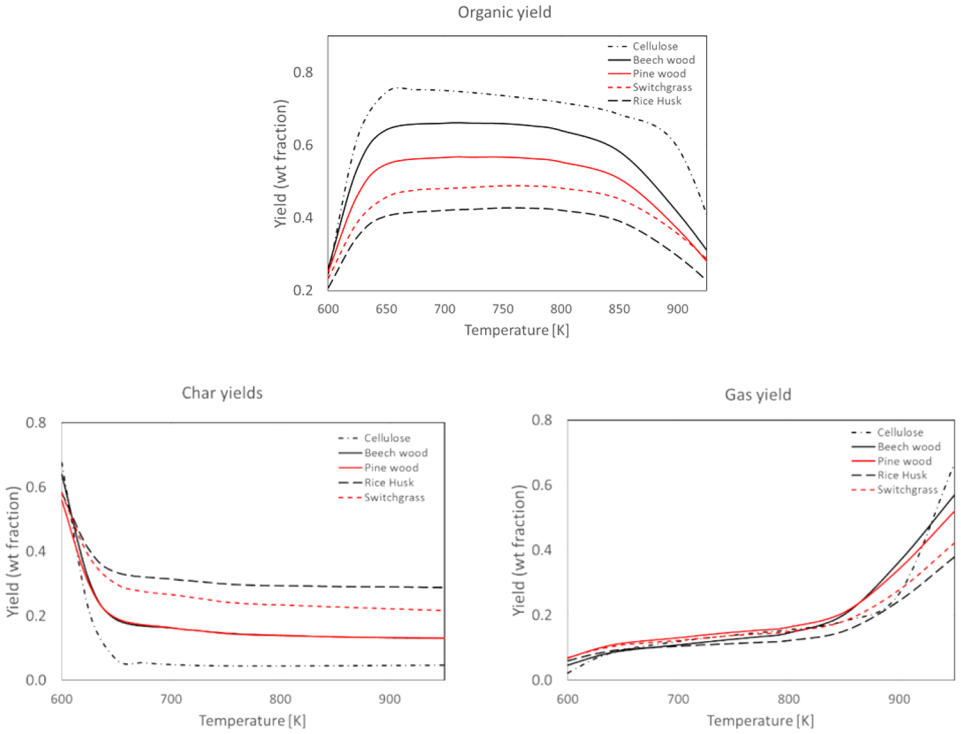

Figure 9. Predicted typical yields of oil, char, and gas from fast pyrolysis of different biomass samples (residence time: solid 5 min, gas 2 s).

water. Deviations between model and experiments are limited and partially contradictory for the two sets of data. In good agreement with experiments, model predicts maximum flat bio-oil yields in a temperature range of ±50 K, for small particles with a complete biomass devolatilization. Carbon oxides are the main gas species from primary pyrolysis, together with small quantities of methane, and ethylene. Primary H_2 yield is very limited and increases at high temperatures, where residual char is nearly constant.

It seems relevant to emphasize the importance, as well as the difficulty, in the complete and correct modeling and simulation of the different reactors. It is first necessary to account for the reactor geometry and conditions, not only in terms of average residence time of gas and solid particles but also in terms of their distribution. Moreover, size distribution of solid particles, together with the characterization of transport properties and heat transfer during the pyrolysis process, are further features to be characterized. The reactor modeling is not in line with the major topics of this work, which mainly relies on the different facets of the chemistry in biomass pyrolysis.

Bio-Oil Yields from Different Biomass Samples. Figure 9 clearly shows that maximum oil content can easily spans between 40% and 80%, mainly because of the different cellulose and hemicellulose content of biomass samples. Biomass with the highest cellulose content gives the maximum bio-oil yields. The occurrence of a maximum in bio-oil yield is due to the partial biomass pyrolysis at low temperatures, and to the successive decomposition reactions of tar species, at high temperatures. Gas yields increase continuously with temperature. At temperatures lower than 700 K, an appropriate residence time (mainly depending on particle dimensions) is essential to complete pyrolysis process and maximize bio-oil yields.

Bio-oil mainly consists of carbohydrates and substituted phenols mostly derived from lignins. Alcohols, aldehydes, furans, and small oxygenated species constitute up to 15−25%, whereas water yield ranges between 10 and 20% of dry biomass. Predicted bio-oil composition agree fairly well with experimental data.[70]

A comprehensive mathematical model of biomass pyrolysis, both at reactor and particle scale, is required to characterize

DOI: 10.1021/acssuschemeng.6b03098
ACS Sustainable Chem. Eng. 2017, 5, 2882−2896

bio-oil formation accounting for the coupling of chemistry and transport processes. In fact, not only the kinetics of pyrolysis reactions, but also the heat and mass diffusivity inside the particle, the heat transfer coefficients, as well as the fluid dynamics inside the reactor, play a crucial role in determining bio-oil production in fast pyrolysis processes.

The yields of organics of Figure 9 refer to average ash conditions, whereas Figure 10 clearly shows the effect of ash on

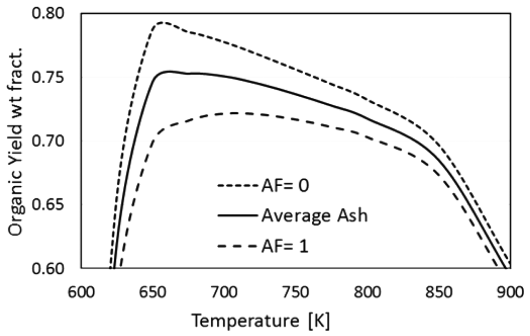

Figure 10. Cellulose pyrolysis: effect of ash on organic yield.

the yield of organics on cellulose pyrolysis. The three yield curves refer to values of ash factor (AF) equal to 0, 0.5, and 1. Because of the ash effect,[1] the maximum of bio-oil spans from 70% to 80 wt % of the original dry biomass.

BIO-OIL COMPOSITION AND COMBUSTION PROPERTIES

As clearly summarized by Lindfors et al.,[71] the properties of fast pyrolysis bio-oils differ significantly from those of fossil fuels. Pyrolysis bio-oil is a dark-brown acidic liquid (pH 2−3) with high water and solid content, and has a heating value that is less than half of hydrocarbon fuels.[72,73] It is possible to increase the heating value only through expensive deoxygenation processes.[74]

Upgrading of Pyrolysis Bio-Oil. Bio-oil is not suitable as transportation fuel without a relevant upgrading. Currently there are two broad approaches for improving the quality of bio-oil. The first one, with typical yields of ∼40%,[73] is based on catalytic processes to eliminate the oxygen in the fuel thus increasing its heating value.[74−77] The catalytic hydro-deoxygenation (HDO) can be alternatively applied to reduce both oxygen content and acidity of bio-oils.[78] The catalytic reactions eliminate oxygen by producing water, while simultaneously decompose and hydrogenate the fuel producing a more conventional hydrocarbon fuel. Compared to catalytic cracking, this process converts about 50% of the original bio-oil. The low liquid yields, the high capital expenses, together with further technical problems, make these catalytic methods less attractive.[73]

The second and more suitable approach to increase the oil quality are based on biomass pretreatment[3,79,80] and physical upgrading. These methods include hot gas filtration, liquid filtration, distillation, and solvent addition. They do not convert bio-oil into a hydrocarbon fuel, but they provide a cheaper and less energy intensive way of improving liquid fuel properties. By far, the simplest and most effective physical upgrading method for bio-oil is the addition of alcohol fuels.

Bio-Oil Composition. The focus of this section is to compare bio-oil with fossil fuels and summarize the challenges in bio-oil combustion resulting both from its physical and chemical characteristics. Bio-oils contain a tar and an aqueous fraction, which makes them immiscible with conventional liquid hydrocarbon fuels. The aqueous fraction contains the low molecular mass (LMM) oxygenated compounds, whereas the tar fraction is constituted by high molecular mass (HMM), water-insoluble lignin fragments (pyrolytic lignin). Bio-oil composition depends on operating conditions and severity of pyrolysis process, as well as on biomass composition. However, bio-oils derived from different biomass streams are more uniform compared to the original biomass resources and have typically 5−20 times higher volumetric energy density. Thus, they potentially decouple liquid fuel production (scale, time, and location) from its utilization, thus improving standardization and market development.[78] This process also enables the separation of residual char and minerals, which can be recycled to the soil as a nutrient. Bio-oils can be used as a fuel or as a renewable raw material for the production of high-value chemicals.[81−83] Recently, Lehto et al.[84] reviewed the existing bio-oil production technologies and compared composition and properties of bio-oil and fossil fuels, as reported in Table S4.

The unusual characteristics of the bio-oil have a great impact on the combustion technology in terms of burner design, flame stability, emissions, and materials compatibility. Fast pyrolysis bio-oils are nonflammable, nondistillable, and possess only limited volatility. In fact, together with water and volatile organic components, they contain substantial amount of nonvolatile materials such as sugars and oligomeric phenolics.[72] Bio-oils are complex mixtures of hundreds of organic compounds that belong to acids, aldehydes, ketones, alcohols, esters, anhydrosugars, furans, phenols, guaiacols, syringols, and nitrogen containing compounds.[85] Figure S4 schematically shows and compares the chemical composition of several bio-oils.[86] Figure 11 satisfactory compares experimental and predicted products yields from the fast pyrolysis of three different typical biomass samples: softwood (pine), hardwood (eucalyptus), and grass. Simulation results refer to pyrolysis

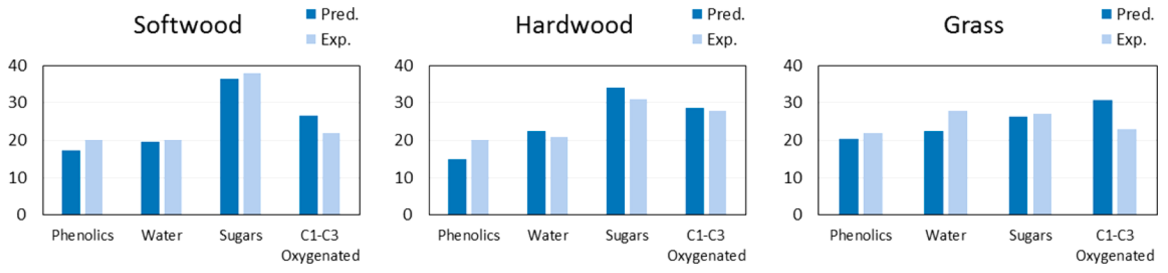

Figure 11. Comparison of experimental[86] and predicted products from the fast pyrolysis of softwood (pine), hardwood (eucalyptus), and grass samples.

DOI: 10.1021/acssuschemeng.6b03098
ACS Sustainable Chem. Eng. 2017, 5, 2882−2896

temperature of 700 K, with a residence time of 2 s for the secondary gas phase reactions of released products.

Combustion of Pyrolysis Bio-Oil and Pollutant Emissions. Bio-oils ignite only at high temperatures, mainly because of the large presence of water and the limited volatility. The low-boiling volatile compounds flash slightly before the evaporated water suppresses ignition. A complete characterization of the distillation curve is not feasible. Bio-oils are not thermally stable: their reactivity already starts below 100 °C and distillation stops at 250−280 °C leaving up to 30−50 wt % of char residue.[69,86,87]

The complexity of the bio-oil composition and the chemical nature of its components are the main reason for the challenging behavior of these fuels in terms of stability, combustion, and corrosion. For these reasons, the existing burners require some modifications to handle the different physical and chemical properties of these alternative biofuels. First, all the parts in contact with bio-oil should be made of stainless steel, and the suitability of all gaskets and instruments needs to be checked. Storage and handling of the bio-oil is also challenging, due to the reactivity and aging of the bio-oil.[69,88]

The quality of biomass pyrolysis oils is inferior to that of conventional fossil fuels, but bio-oil characteristics can be improved by adding polar solvents, such as methanol and ethanol. Alcohol addition has a beneficial effect on the storage stability, reduces the viscosity and promotes ignition and flame stability. In fact, bio-oils are mainly composed by scarcely volatile components and significant energy is required for ignition. Bio-oil flames have a similar or longer flame length compared to conventional fossil fuels.[89] Visual observations of bio-oil flames indicate the presence of a stable combustion zone followed by a region where char particles formed from individual droplets undergo burnout.[87,90] The flame length and stability depends on a number of factors, including atomization quality, fuelling rate, spray inlet velocity, flame swirl, and recirculation.

Green house gases (GHG), NO_x, polycyclic hydrocarbon aromatics, and soot are the typical combustion pollutants. Although the emissions of CO_2 mainly depend on the renewable fuel integral production process, the formation of the other pollutants depends on the combustor device characteristics and fuel composition. Pollutants formation is a major issue for bio-oil combustion. Emissions are very dependent on the levels of solids, ash, water, nitrogen, and sulfur in the oil being combusted. Typically, the emissions levels are between those of light fuel oil (LFO) and the lightest heavy fuel oil (HFO), but particulate emission may be higher.[91,92] NO_x emissions are mostly associated with the nitrogen content of bio-oil, which is typically of the order of 0.1−0.9%.[93,94]

Because of the low sulfur amount in biomass compared to fossil fuels, SO_x emissions are practically absent in bio-oil combustion. PAH and particulate emissions depend on the relative role of reactions in the gas and liquid phases.[86]

The combustion process of a pyrolysis oil droplet starts with the evaporation of water, followed by the selective evaporation of light compounds, whereas the heavier components can also undergo a significant liquid-phase pyrolysis. This pyrolysis process can lead to the formation of a carbonaceous shell at the droplet surface, associated with swelling of the droplet and microexplosions, and ultimately to the formation of a solid residue in the form of carbonaceous Cenospheres.[95−97] Therefore, a sufficiently large residence time of spray droplets in the hot combustion zone of the flame is needed to promote the burnout of solid residues,[84] and the kinetics of the residual char burnout needs to be taken into account. Conventional soot mechanisms contribute only partially to the total particulate emissions.[73]

It is therefore necessary to develop models able to predict not only the complex evaporation of a bio-oil droplets but also its combustion kinetics, including pollutant formation, as well as char formation and particle burnout. From a kinetic modeling perspective, the description of the combustion of bio-oil is a very complex task at least for three different reasons. The first one is the challenging characterization of these mixtures of several components. The second is the complexity of the oxidation mechanism of large molecules such as carboxylic acids, sugars, and heavy substituted phenol species derived from pyrolytic lignins. Finally, the third one is that the initial combustion of volatile LMM compounds, that readily evaporate from the droplet, is followed by polymerization and pyrolysis reactions of the HMM compounds in the liquid phase with the possible formation of a char residue in the form of Cenospheres.

CONCLUSION

A comprehensive and unifying mathematical model to describe the chemistry of fast biomass pyrolysis is discussed in this paper. Emphasis is given to the multicomponent, multiphase, multiscale nature of this problem, together with the several simplifications for both the gas and solid phase kinetic mechanisms. The overall model is completely predictive and only requires the ultimate biomass analysis. The biomass characterization through a limited number of reference components is only the first step of this process. To reduce the complexity of the overall system, lumping procedures are applied to describe the chemical evolution toward the formation of bio-oil. Similar simplifications are also applied to the secondary gas-phase reactions. Finally, the coupling of the kinetic mechanisms with mass and energy transport resistances at particle and reactor scale constitutes a further difficulty.

The satisfactory comparisons with experimental data prove the model reliability, despite the oversimplifications required for an effective use of the model at the reactor scale. Since the original formulation, the model has been progressively extended, and now it includes the distinction between hardwood and softwood biomass samples as well as the catalytic effect of ash. It is relevant to underline that mainly the biomass pyrolysis model remains a first attempt to describe the complex behavior of pyrolysis products. Despite these simplifications, this model is the only one, to our knowledge, able to describe the chemistry of the whole process from biomass to bio-oil in a predictive and satisfactory way.

Five years ago, Mettler et al.[8] already identified the ten major research features and challenges useful for a more fundamental understanding of biomass pyrolysis and a better design of fast pyrolysis process. These issues, partially discussed in this work, can be summarized at least in the following four topics:

1. Characterization and chemistry of the biomass pyrolysis.
   a. Interactions of the released products within the intermediate liquid and the gas phase.
   b. Primary and secondary char formation.
   c. Catalytic effects of inorganic species.
2. Biomass particle model.
   a. Transport properties, porosity, and particle shrinkage

DOI: 10.1021/acssuschemeng.6b03098
ACS Sustainable Chem. Eng. 2017, 5, 2882−2896

b. Aerosol formation and bio-oil properties.

3. Heat transfer and reactor model

4. New analytical techniques and experimental activities useful to validate the overall models.

Recent and intensive theoretical and experimental activities on cellulose, hemicellulose, and lignin pyrolysis mechanisms, also including catalytic effect of ash, give a satisfactory answer to the first of these points. The second critical feature mainly relates to the complex biomass structure of directional pores, which impacts heat and mass transfer within particles during conversion processes. On the basis of measurements of microstructural particle size and morphology, including cell wall thickness and cell lumen dimensions, Ciesielski et al.[98] presented a general algorithm that produces representative geometrical models of biomass particles. Moreover, they analyzed different biomass particles demonstrating the utility of finite element simulations to better describe intraparticle heat and mass transfer. Similarly, Gentile et al.[99] presented a new computational framework for modeling the pyrolysis of anisotropic biomass particles. These models account for the particle shrinking and can give a better insight into the relative role and time evolution of transport phenomena and chemical kinetics.

From an experimental point of view, Paulsen et al.[100] proposed a new experimental technique capable of measuring biomass composition during fast pyrolysis with high spatial and temporal resolution. They also compared compositional data with a comprehensive 2D single particle model, which incorporated a multistep reaction mechanism, prescribed particle shrinkage, and variable thermophysical properties. This technique highlights the relative role of the chemistry and the transport processes in biomass pyrolysis. Moreover, important analytical efforts are spent to characterize pyrolysis bio-oil. Thus, Negahdar et al.[101] identified and quantified 200 individual compounds using quantitative ^{13}C nuclear magnetic resonance combined with comprehensive two-dimensional gas chromatography. Similarly, slow and fast biomass pyrolysis was investigated both on fluidized and fixed bed reactors combined with a single photoionization mass spectrometer.[102,103] Final yields of permanent gases and major primary tars are measured by GC analysis, whereas the soft ionization capability allows real-time and online analysis of the labile primary tars.[104] Although these and similar research activities contribute to elucidate the longstanding challenges in the development of fast pyrolysis models and technology, still future experimental and theoretical works are required for further validation and extension of comprehensive models of fast pyrolysis process.

Even if the pyrolysis mechanisms and the reactor modeling still require further research efforts, from a process viewpoint we can conclude that biomass pyrolysis to bio-oil currently reached a mature stage of development with several technologies already achieving full commercialization stage.[2,3]

■ ASSOCIATED CONTENT

Supporting Information

The Supporting Information is available free of charge on the ACS Publications website at DOI: 10.1021/acssuschemeng.6b03098.

POLIMI kinetic mechanism of secondary pyrolysis reactions in CHEMKIN format: Figure S1 schematically shows a fast pyrolysis process[2]; Figure S2 shows the rate constants of H-abstraction reactions of H, OH, and CH_3; Figure S3 displays the dehydration reactions of 2-butanol to form butenes; Figure S4 reports and compares the compositions of different biomass samples; Table S1 summarizes the multistep kinetic scheme of biomass pyrolysis, and Table S2 reports the formation enthalpy and entropy of major biomass pyrolysis products; Table S3 reports the operating conditions of biomass thermal treatments; Table S4 compares main properties of bio-oil, heavy fuel oil, and light fuel oil[81] (PDF)

Secondary, gas-phase kinetic mechanism in CHEMKIN format (TXT)

Thermo properties (TXT)

Names of components (TXT)

■ AUTHOR INFORMATION

Corresponding Author

*E. Ranzi. Phone: +39 (0)2 2399 3250; Fax: +39 (0)2 7063 8173; Email: eliseo.ranzi@polimi.it.

ORCID

Eliseo Ranzi: 0000-0002-1395-6074

Notes

The authors declare no competing financial interest.

■ ACKNOWLEDGMENTS

A.F. acknowledges the support by the European Union's Horizon 2020 research and innovation programme (Residue2-Heat project, G.A. No. 654650). P.D. gratefully acknowledges the financial support from CAPES Foundation, Ministry of Education of Brazil−Science without Borders Mobility Program−Full Ph.D. Scholarship Process No. 10131/13-2. This paper summarizes the research activities on biomass pyrolysis done at CMIC Department of Politecnico di Milano. The contributions of all the friends, colleagues, and Ph.D. and Master's students are gratefully acknowledged. Particularly, the authors acknowledge the very useful works, discussions, and comments of Prof. M. Dente, S. Pierucci, T. Faravelli, A. Cuoci, and F. Manenti.

■ REFERENCES

(1) Ranzi, E.; Debiagi, P. E. A.; Frassoldati, A. Mathematical modeling of fast biomass pyrolysis and bio-oil formation. Note I: Kinetic mechanism of biomass pyrolysis. *ACS Sustainable Chem. Eng.* **2017**, DOI: 10.1021/acssuschemeng.6b03096.

(2) Bridgwater, A. V. Review of fast pyrolysis of biomass and product upgrading. *Biomass Bioenergy* **2012**, *38*, 68−94.

(3) Kan, T.; Strezov, V.; Evans, T. J. Lignocellulosic biomass pyrolysis: A review of product properties and effects of pyrolysis parameters. *Renewable Sustainable Energy Rev.* **2016**, *57*, 1126−1140.

(4) Ranzi, E.; Corbetta, M.; Manenti, F.; Pierucci, S. Kinetic modeling of the thermal degradation and combustion of biomass. *Chem. Eng. Sci.* **2014**, *110*, 2−12.

(5) Dente, M.; Ranzi, E.; Goossens, A. G. Detailed prediction of olefin yields from hydrocarbon pyrolysis through a fundamental simulation model (SPYRO). *Comput. Chem. Eng.* **1979**, *3*, 61−75.

(6) Ranzi, E.; Sogaro, A.; Gaffuri, P.; Pennati, G.; Westbrook, C. K.; Pitz, W. J. A new comprehensive reaction mechanism for combustion of hydrocarbon fuels. *Combust. Flame* **1994**, *99* (2), 201−211.

(7) Carstensen, H. H.; Dean, A. M. Development of detailed kinetic models for the thermal conversion of biomass via first principle methods and rate estimation rules. Computational Modeling in Lignocellulosic Biofuel Production. *ACS Symp. Ser.* **2010**, *1052*, 201−243.

(8) Mettler, M. S.; Vlachos, D. G.; Dauenhauer, P. J. Top ten fundamental challenges of biomass pyrolysis for biofuels. *Energy Environ. Sci.* **2012**, *5*, 7797−7809.
(9) Debiagi, P. E. A.; Gentile, G.; Pelucchi, M.; Frassoldati, A.; Cuoci, A.; Faravelli, T.; Ranzi, E. Detailed kinetic mechanism of gas-phase reactions of volatiles released from biomass pyrolysis. *Biomass Bioenergy* **2016**, *93*, 60−71.
(10) Bridgwater, A. V. Renewable fuels and chemicals by thermal processing of biomass. *Chem. Eng. J.* **2003**, *91*, 87−102.
(11) Di Blasi, C. Modeling chemical and physical processes of wood and biomass pyrolysis. *Prog. Energy Combust. Sci.* **2008**, *34*, 47−90.
(12) Di Blasi, C. Combustion and gasification rates of lignocellulosic chars. *Prog. Energy Combust. Sci.* **2009**, *35* (2), 121−140.
(13) Calonaci, M.; Grana, R.; Barker Hemings, E.; Bozzano, G.; Dente, M.; Ranzi, E. Comprehensive kinetic modeling study of bio-oil formation from fast pyrolysis of biomass. *Energy Fuels* **2010**, *24* (10), 5727−5734.
(14) Ranzi, E.; Frassoldati, A.; Grana, R.; Cuoci, A.; Faravelli, T.; Kelley, A.; Law, C. Hierarchical and comparative kinetic modeling of laminar flame speeds of hydrocarbon and oxygenated fuels. *Prog. Energy Combust. Sci.* **2012**, *38* (4), 468−501.
(15) Rodriguez, A.; Herbinet, O.; Battin-Leclerc, F.; Frassoldati, A.; Faravelli, T.; Ranzi, E. Experimental and modeling investigation of the effect of the unsaturation degree on the gas-phase oxidation of fatty acid methyl esters found in biodiesel fuels. *Combust. Flame* **2016**, *164*, 346−36.
(16) Dente, M.; Pierucci, S.; Ranzi, E.; Bussani, G. New improvements in modeling kinetic schemes for hydrocarbons pyrolysis reactors. *Chem. Eng. Sci.* **1992**, *47* (9), 2629−2634.
(17) Ranzi, E.; Dente, M.; Faravelli, T.; Pennati, G. Prediction of kinetic parameters for hydrogen abstraction reactions. *Combust. Sci. Technol.* **1993**, *95* (1−6), 1−50.
(18) Pelucchi, M.; Cavallotti, C.; Ranzi, E.; Frassoldati, A.; Faravelli, T. Relative reactivity of oxygenated fuels: alcohols, aldehydes, ketons and methyl esters. *Energy Fuels* **2016**, *30* (10), 8665−8679.
(19) Vinu, R.; Broadbelt, L. J. A mechanistic model of fast pyrolysis of glucose-based carbohydrates to predict bio-oil composition. *Energy Environ. Sci.* **2012**, *5* (12), 9808−9826.
(20) Seshadri, V.; Westmoreland, P. R. Concerted Reactions and Mechanism of Glucose Pyrolysis and Implications for Cellulose Kinetics. *J. Phys. Chem. A* **2012**, *116*, 11997−12013.
(21) Zhou, X.; Nolte, M. W.; Mayes, H. B.; Shanks, B. H.; Broadbelt, L. J. Experimental and mechanistic modeling of fast pyrolysis of neat glucose-based carbohydrates. 1. Experiments and development of a detailed mechanistic model. *Ind. Eng. Chem. Res.* **2014**, *53* (34), 13274−13289.
(22) Frassoldati, A.; Cuoci, A.; Faravelli, T.; Niemann, U.; Ranzi, E.; Seiser, R.; Seshadri, K. An experimental and kinetic modeling study of n-propanol and iso-propanol combustion. *Combust. Flame* **2010**, *157* (1), 2−16.
(23) Grana, R.; Frassoldati, A.; Faravelli, T.; Niemann, U.; Ranzi, E.; Seiser, R.; Cattolica, R.; Seshadri, K. An experimental and kinetic modeling study of combustion of isomers of butanol. *Combust. Flame* **2010**, *157* (11), 2137−2154.
(24) Sarathy, S. M.; Oßwald, P.; Hansen, N.; Kohse-Höinghaus, K. Alcohol combustion chemistry. *Prog. Energy Combust. Sci.* **2014**, *44*, 40−102.
(25) Fantozzi, F.; Frassoldati, A.; Bartocci, P.; Cinti, G.; Quagliarini, F.; Bidini, G.; Ranzi, E. M. An experimental and kinetic modeling study of glycerol pyrolysis. *Appl. Energy* **2016**, *184*, 68−76.
(26) Fukutome, A.; Kawamoto, H.; Saka, S. Gas-Phase Reactions of Glyceraldehyde and 1, 3-Dihydroxyacetone as Models for Levoglucosan Conversion during Biomass Gasification. *ChemSusChem* **2016**, *9* (7), 703−712.
(27) Kawasaki, K.; Yamane, K. Thermal Decomposition of Waste Glycerol. *Proceedings of the International Conference on Power Engineering-09 (ICOPE-09)*, November 16−20, 2009, Kobe, Japan.
(28) Shin, E. J.; Nimlos, M. R.; Evans, R. J. Kinetic analysis of the gas-phase pyrolysis of carbohydrates. *Fuel* **2001**, *80* (12), 1697−1709.
(29) Shen, D.; Jin, W.; Hu, J.; Xiao, R.; Luo, K. An overview on fast pyrolysis of the main constituents in lignocellulosic biomass to valued-added chemicals: Structures, pathways and interactions. *Renewable Sustainable Energy Rev.* **2015**, *51*, 761−774.
(30) Ranzi, E.; Faravelli, T.; Gaffuri, P.; Garavaglia, E.; Goldaniga, A. Primary pyrolysis and oxidation reactions of linear and branched alkanes. *Ind. Eng. Chem. Res.* **1997**, *36* (8), 3336−3344.
(31) Kawamoto, H.; Murayama, M.; Saka, S. Pyrolysis behavior of levoglucosan as an intermediate in cellulose pyrolysis: polymerization into polysaccharide as a key reaction to carbonized product formation. *J. Wood Sci.* **2003**, *49* (5), 469−473.
(32) Fukutome, A.; Kawamoto, H.; Saka, S. Processes forming Gas, Tar, and Coke in Cellulose Gasification from Gas-Phase Reactions of Levoglucosan as Intermediate. *ChemSusChem* **2015**, *8* (13), 2240−2249.
(33) Organ, P. P.; Mackie, J. C. Kinetics of pyrolysis of furan. *J. Chem. Soc., Faraday Trans.* **1991**, *87* (6), 815−823.
(34) Sendt, K.; Bacskay, G. B.; Mackie, J. C. Pyrolysis of furan: Ab initio quantum chemical and kinetic modeling studies. *J. Phys. Chem. A* **2000**, *104* (9), 1861−1875.
(35) Wei, L.; Tang, C.; Man, X.; Huang, Z. Shock-tube experiments and kinetic modeling of 2-methylfuran ignition at elevated pressure. *Energy Fuels* **2013**, *27* (12), 7809−7816.
(36) Liu, D.; Togbé, C.; Tran, L. S.; Felsmann, D.; Oßwald, P.; Nau, P.; Fournet, R.; Koppmann, J.; Lackner, A.; Glaude, P.-A.; Sirjean, B.; Battin-Leclerc, F.; Kohse-Höinghaus, F. Combustion chemistry and flame structure of furan group biofuels using molecular-beam mass spectrometry and gas chromatography−Part I: Furan. *Combust. Flame* **2014**, *161* (3), 748−765.
(37) Somers, K. P.; Simmie, J. M.; Metcalfe, W. K.; Curran, H. J. The pyrolysis of 2-methylfuran: a quantum chemical, statistical rate theory and kinetic modelling study. *Phys. Chem. Chem. Phys.* **2014**, *16* (11), 5349−5367.
(38) Pecullan, M.; Brezinsky, K.; Glassman, I. Pyrolysis and oxidation of anisole near 1000 K. *J. Phys. Chem. A* **1997**, *101* (18), 3305−3316.
(39) Barker-Hemings, E.; Bozzano, G.; Dente, M.; Ranzi, E. Detailed kinetics of the pyrolysis and oxidation of anisole. *Chem. Eng. Trans.* **2011**, *24*, 61−66.
(40) Nowakowska, M.; Herbinet, O.; Dufour, A.; Glaude, P. A. Detailed kinetic study of anisole pyrolysis and oxidation to understand tar formation during biomass combustion and gasification. *Combust. Flame* **2014**, *161* (6), 1474−1488.
(41) Kotake, T.; Kawamoto, H.; Saka, S. Pyrolytic formation of monomers from hardwood lignin as studied from the reactivities of the primary products. *J. Anal. Appl. Pyrolysis* **2015**, *113*, 57−64.
(42) Norinaga, K.; Yang, H.; Tanaka, R.; Appari, S.; Iwanaga, K.; Takashima, Y.; Hayashi, J. I.; Kudo, S.; Shoji, T. A mechanistic study on the reaction pathways leading to benzene and naphthalene in cellulose vapor phase cracking. *Biomass Bioenergy* **2014**, *69*, 144−154.
(43) Frenklach, M.; Wang, H. Detailed modeling of soot particle nucleation and growth. In *Symposium (International) on Combustion*; Elsevier: Amsterdam, 1991; Vol. *23*, No. 1, pp 1559−1566.
(44) D'Alessio, A.; D'Anna, A.; D'orsi, A.; Minutolo, P.; Barbella, R.; Ciajolo, A. Precursor formation and soot inception in premixed ethylene flames. In *Symposium (International) on Combustion*; Elsevier: Amsterdam, 1992; Vol. *24*, No. 1, pp 973−980.
(45) Djokic, M. R.; Van Geem, K. M.; Cavallotti, C.; Frassoldati, A.; Ranzi, E.; Marin, G. B. An experimental and kinetic modeling study of cyclopentadiene pyrolysis: First growth of polycyclic aromatic hydrocarbons. *Combust. Flame* **2014**, *161* (11), 2739−2751.
(46) Saggese, C.; Ferrario, S.; Camacho, J.; Cuoci, A.; Frassoldati, A.; Ranzi, E.; Wang, H.; Faravelli, T. Kinetic modeling of particle size distribution of soot in a premixed burner-stabilized stagnation ethylene flame. *Combust. Flame* **2015**, *162* (9), 3356−3369.
(47) Norinaga, K.; Shoji, T.; Kudo, S.; Hayashi, J. I. Detailed chemical kinetic modelling of vapour-phase cracking of multi-component molecular mixtures derived from the fast pyrolysis of cellulose. *Fuel* **2013**, *103*, 141−150.

DOI: 10.1021/acssuschemeng.6b03098
ACS Sustainable Chem. Eng. 2017, 5, 2882−2896

(48) Corbetta, M.; Frassoldati, A.; Bennadji, H.; Smith, K.; Serapiglia, M. J.; Gauthier, G.; Melkior, T.; Ranzi, E.; Fisher, E. M. Pyrolysis of centimeter-scale woody biomass particles: Kinetic modeling and experimental validation. *Energy Fuels* **2014**, *28* (6), 3884−3898.
(49) Yang, H. M.; Appari, S.; Kudo, S.; Hayashi, J. I.; Norinaga, K. Detailed Chemical Kinetic Modeling of Vapor-Phase Reactions of Volatiles Derived from Fast Pyrolysis of Lignin. *Ind. Eng. Chem. Res.* **2015**, *54* (27), 6855−6864.
(50) Neves, D.; Thunman, H.; Matos, A.; Tarelho, L.; Gómez-Barea, A. Characterization and prediction of biomass pyrolysis products. *Prog. Energy Combust. Sci.* **2011**, *37* (5), 611−630.
(51) Asadullah, M.; Zhang, S.; Min, Z.; Yimsiri, P.; Li, C. Z. Effects of biomass char structure on its gasification reactivity. *Bioresour. Technol.* **2010**, *101* (20), 7935−7943.
(52) Klinghoffer, N. B.; Castaldi, M. J.; Nzihou, A. Catalyst properties and catalytic performance of char from biomass gasification. *Ind. Eng. Chem. Res.* **2012**, *51* (40), 13113−13122.
(53) Lv, D.; Xu, M.; Liu, X.; Zhan, Z.; Li, Z.; Yao, H. Effect of cellulose, lignin, alkali and alkaline earth metallic species on biomass pyrolysis and gasification. *Fuel Process. Technol.* **2010**, *91* (8), 903−909.
(54) Froment, G. F.; Bischoff, K. B. *Chemical reactor analysis and design*; John Wiley & Sons: New York, 1990.
(55) Griffiths, J. F.; Barnard, J. A. *Flame and combustion*; Chapman & Hall: London, U. K., 1995.
(56) Di Blasi, C. Modeling and simulation of combustion processes of charring and non-charring solid fuels. *Prog. Energy Combust. Sci.* **1993**, *19*, 71−104.
(57) Groeneveld, M. J.; Van Swaaij, W. P. M. Gasification of char particles with CO2 and H2O. *Chem. Eng. Sci.* **1980**, *35*, 307−313.
(58) Tognotti, L.; Longwell, J. P.; Sarofim, A. F. The products of the high temperature oxidation of a single char particle in an electrodynamic balance. *Symp. (Int.) Combust., [Proc.]* **1991**, *23*, 1207−1213.
(59) Di Blasi, C.; Branca, C.; Sarnataro, F. E.; Gallo, A. Thermal runaway in the pyrolysis of some lignocellulosic biomasses. *Energy Fuels* **2014**, *28* (4), 2684−2696.
(60) Park, W. C.; Atreya, A.; Baum, H. R. Experimental and theoretical investigation of heat and mass transfer processes during wood pyrolysis. *Combust. Flame* **2010**, *157* (3), 481−494.
(61) Ranzi, E.; Pierucci, S.; Aliprandi, P. C.; Stringa, S. Comprehensive and detailed kinetic model of a traveling grate combustor of biomass. *Energy Fuels* **2011**, *25* (9), 4195−4205.
(62) Mohan, D.; Pittman, C. U.; Steele, P. H. Pyrolysis of wood/biomass for bio-oil: a critical review. *Energy Fuels* **2006**, *20* (3), 848−889.
(63) Van der Stelt, M. J. C.; Gerhauser, H.; Kiel, J. H. A.; Ptasinski, K. J. Biomass upgrading by torrefaction for the production of biofuels: A review. *Biomass Bioenergy* **2011**, *35* (9), 3748−3762.
(64) Shankar Tumuluru, J.; Sokhansanj, S.; Hess, J. R.; Wright, C. T.; Boardman, R. D. REVIEW: A review on biomass torrefaction process and product properties for energy applications. *Ind. Biotechnol.* **2011**, *7* (5), 384−401.
(65) Wagenaar, B. M.; Venderbosch, R. H.; Carrasco, J.; Strenziok, R.; van der Aa, B. J. Rotating cone bio-oil production and applications. In *Progress in thermochemical biomass conversion*; Bridgwater, A. V., Ed.; Blackwell Science: Oxford, U. K., 2001; pp 1268−1280.
(66) Meier, D.; van de Beld, B.; Bridgwater, A. V.; Elliott, D. C.; Oasmaa, A.; Preto, F. State-of-the-art of fast pyrolysis in IEA bioenergy member countries. *Renewable Sustainable Energy Rev.* **2013**, *20*, 619−641.
(67) Aguado, R.; Olazar, M.; San José, M. J.; Aguirre, G.; Bilbao, J. Pyrolysis of sawdust in a conical spouted bed reactor. Yields and product composition. *Ind. Eng. Chem. Res.* **2000**, *39* (6), 1925−1933.
(68) Olazar, M.; Aguado, R.; Bilbao, J.; Barona, A. Pyrolysis of sawdust in a conical spouted-bed reactor with a HZSM-5 catalyst. *AIChE J.* **2000**, *46* (5), 1025−1033.
(69) Westerhof, R. J.; Brilman, D. W.; van Swaaij, W. P.; Kersten, S. R. Effect of temperature in fluidized bed fast pyrolysis of biomass: oil quality assessment in test units. *Ind. Eng. Chem. Res.* **2010**, *49* (3), 1160−1168.
(70) Oasmaa, A.; Sundqvist, T.; Kuoppala, E.; Garcia-Perez, M.; Solantausta, Y.; Lindfors, C.; Paasikallio, V. Controlling the phase stability of biomass fast pyrolysis bio-oils. *Energy Fuels* **2015**, *29* (7), 4373−4381.
(71) Lindfors, C.; Kuoppala, E.; Oasmaa, A.; Solantausta, Y.; Arpiainen, V. Fractionation of bio-oil. *Energy Fuels* **2014**, *28* (9), 5785−5791.
(72) Oasmaa, A.; Czernik, S. Fuel Oil Quality of Biomass Pyrolysis Oils - State of the Art for the End Users. *Energy Fuels* **1999**, *13*, 914−92.
(73) Tzanetakis, T.; Moloodi, S.; Farra, N.; Nguyen, B.; Thomson, M. J. Spray Combustion and Particulate Matter Emissions of a Wood Derived Fast Pyrolysis Liquid-Ethanol Blend in a Pilot Stabilized Swirl Burner. *Energy Fuels* **2011**, *25*, 1405−1422.
(74) Ringer, M.; Putsche, V.; Scahill, J. *Large-Scale Pyrolysis Oil Production: A Technology Assessment and Economic Analysis*; Technical Report NREL/TP-510-37779; National Renewable Energy Laboratory: Golden, CO, 2006.
(75) Czernik, S.; Bridgwater, A. V. Overview of applications of biomass fast pyrolysis oil. *Energy Fuels* **2004**, *18* (2), 590−598.
(76) Maggi, R. E.; Elliot, D. C. Upgrading overview. In *Developments in Thermochemical Biomass Conversion*; Bridgwater, A. V.; Boocock, D. G. B., Eds.; Springer: Dordrecht, The Netherlands, 1997; Vol. *1*, pp 575−588, DOI: 10.1007/978-94-009-1559-6_45.
(77) Mortensen, P. M.; Grunwaldt, J. D.; Jensen, P. A.; Knudsen, K. G.; Jensen, A. D. A review of catalytic upgrading of bio-oil to engine fuels. *Appl. Catal., A* **2011**, *407*, 1−19.
(78) Marsman, J. H.; Wildschut, J.; Mahfud, F.; Heeres, H. J. Identification of components in fast pyrolysis oil and upgraded products by comprehensive two-dimensional gas chromatography and flame ionisation detection. *J. Chromatogr. A* **2007**, *1150*, 21−27.
(79) Banks, S. W.; Nowakowski, D. J.; Bridgwater, A. V. Fast pyrolysis processing of surfactant washed Miscanthus. *Fuel Process. Technol.* **2014**, *128*, 94−103.
(80) Banks, S. W.; Nowakowski, D. J.; Bridgwater, A. V. Impact of potassium and phosphorus in biomass on the properties of fast pyrolysis bio-oil. *Energy Fuels* **2016**, *30* (10), 8009−8018.
(81) Venderbosch, R.; Prins, W. Fast pyrolysis technology development. *Biofuels, Bioprod. Biorefin.* **2010**, *4*, 178−208.
(82) Kim, J. S. Production, separation and applications of phenolic-rich bio-oil−A review. *Bioresour. Technol.* **2015**, *178*, 90−98.
(83) Toraman, H. E.; Vanholme, R.; Borén, E.; Vanwonterghem, Y.; Djokic, M. R.; Yildiz, G.; Ronsse, F.; Prins, W.; Boerjan, W.; Van Geem, K. M.; Marin, G. B. Potential of genetically engineered hybrid poplar for pyrolytic production of bio-based phenolic compounds. *Bioresour. Technol.* **2016**, *207*, 229−236.
(84) Lehto, J.; Oasmaa, A.; Solantausta, Y.; Kytö, M.; Chiaramonti, D. Review of fuel oil quality and combustion of fast pyrolysis bio-oils from lignocellulosic biomass. *Appl. Energy* **2014**, *116*, 178−190.
(85) Djokic, M. R.; Dijkmans, T.; Yildiz, G.; Prins, W.; Van Geem, K. M. Quantitative analysis of crude and stabilized bio-oils by comprehensive two-dimensional gas-chromatography. *Journal of Chromatography A* **2012**, *1257*, 131−140.
(86) Oasmaa, A.; Solantausta, Y.; Arpiainen, V.; Kuoppala, E.; Sipilä, K. Fast Pyrolysis Bio-Oils from Wood and Agricultural Residues. *Energy Fuels* **2010**, *24*, 1380−1388.
(87) Krumdieck, S. P.; Daily, J. W. Evaluating the feasibility of biomass pyrolysis oil for spray combustion applications. *Combust. Sci. Technol.* **1998**, *134*, 351−365.
(88) Czernik, S.; Johnson, D. K.; Black, S. Stability of Wood fast Pyrolysis Oil. *Biomass Bioenergy* **1994**, *7*, 187−192.
(89) Czernik, S.; Bridgwater, A. V. Overview of applications of biomass fast pyrolysis oil. *Energy Fuels* **2004**, *18* (2), 590−598.
(90) Stamatov, V.; Honnery, D.; Soria, J. Combustion properties of slow pyrolysis bio-oil produced from indigenous Australian species. *Renewable Energy* **2006**, *31*, 2108−2121.

DOI: 10.1021/acssuschemeng.6b03098
ACS Sustainable Chem. Eng. 2017, 5, 2882−2896

(91) Oasmaa, A.; Kytö, M.; Sipilä, K. Pyrolysis liquid combustion tests in an industrial boiler. In *Progress in thermochemical biomass conversion*; Bridgwater, A., Ed.; Blackwell Science, Oxford, U. K., 2001; Vol. 2, pp 1468−1481.
(92) Solantausta, Y.; Oasmaa, A.; Sipilä, K.; Lindfors, C.; Lehto, J.; Autio, J.; Jokela, P.; Alin, J.; Heiskanen, J. Bio-oil production from biomass: steps toward demonstration. *Energy Fuels* **2012**, *26* (1), 233−240.
(93) Khodier, A.; Kilgallon, P.; Legrave, N.; Simms, N.; Oakey, J.; Bridgwater, T. Pilot-scale combustion of fast-pyrolysis bio-oil: ash deposition and gaseous emissions. *Environ. Prog. Sustainable Energy* **2009**, *28* (3), 397−403.
(94) No, S. Y. Application of bio-oils from lignocellulosic biomass to transportation, heat and power generation - A review. *Renewable Sustainable Energy Rev.* **2014**, *40*, 1108−1125.
(95) Calabria, R.; D'Alessio, A.; Lazzaro, M.; Massoli, P.; Moccia, V. High pressure combustion of wood pyrolysis oil. *SAE Tech. Pap. Ser.* **2001**, 24−0025.
(96) Wornat, M. J.; Porter, B. G.; Yang, N. Y. C. Single Droplet Combustion of Biomass Pyrolysis Oils. *Energy Fuels* **1994**, *8*, 1131−1142.
(97) Balegedde Ramachandran, R. P.; van Rossum, G.; van Swaaij, W. P. M.; Kersten, S. R. A. Evaporation of Biomass Fast Pyrolysis Oil: Evaluation of Char Formation. *Environ. Prog. Sustainable Energy* **2009**, *28* (3), 410−417.
(98) Ciesielski, P. N.; Crowley, M. F.; Nimlos, M. R.; Sanders, A. W.; Wiggins, G. M.; Robichaud, D.; Donohoe, B. S.; Foust, T. D. Biomass particle models with realistic morphology and resolved microstructure for simulations of intraparticle transport phenomena. *Energy Fuels* **2015**, *29* (1), 242−254.
(99) Gentile, G.; Debiagi, P. E. A; Cuoci, A.; Frassoldati, A.; Ranzi, E.; Faravelli, T. A computational framework for the pyrolysis of anisotropic biomass particles. *Chem. Eng. J.* **2017**, submitted.
(100) Paulsen, A. D.; Hough, B. R.; Williams, C. L.; Teixeira, A. R.; Schwartz, D. T.; Pfaendtner, J.; Dauenhauer, P. J. Fast pyrolysis of wood for biofuels: spatio-temporally resolved diffuse reflectance in situ spectroscopy of particles. *ChemSusChem* **2014**, *7* (3), 765−776.
(101) Negahdar, L.; Gonzalez-Quiroga, A.; Otyuskaya, D.; Toraman, H. E.; Liu, L.; Jastrzebski, J. T.; Van Geem, K. M.; Marin, G. B.; Thybaut, J. W.; Weckhuysen, B. M. Characterization and Comparison of Fast Pyrolysis Bio-oils from Pinewood, Rapeseed Cake, and Wheat Straw Using 13C NMR and Comprehensive GC × GC. *ACS Sustainable Chem. Eng.* **2016**, *4* (9), 4974−4985.
(102) Jia, L.; Le Brech, Y.; Mauviel, G.; Qi, F.; Bente-von Frowein, M.; Ehlert, S.; Zimmermann, R.; Dufour, A. Online analysis of biomass pyrolysis tar by photoionization mass spectrometry. *Energy Fuels* **2016**, *30* (3), 1555−1563.
(103) Jia, L.; Dufour, A.; Le Brech, Y.; Authier, O.; Mauviel, G. On-line analysis of primary tars from biomass pyrolysis by single photoionization mass spectrometry: Experiments and detailed modelling. *Chem. Eng. J.* **2017**, *313*, 270−282.
(104) Le Brech, Y.; Jia, L.; Cissé, S.; Mauviel, G.; Brosse, N.; Dufour, A. Mechanisms of biomass pyrolysis studied by combining a fixed bed reactor with advanced gas analysis. *J. Anal. Appl. Pyrolysis* **2016**, *117*, 334−346.

DOI: 10.1021/acssuschemeng.6b03098
ACS Sustainable Chem. Eng. 2017, 5, 2882−2896